Available online at www.sciencedirect.com
SCIENCE DIRECT
Journal of Magnetic Resonance 181 (2006) 79–88
JMR Journal of Magnetic Resonance
www.elsevier.com/locate/jmr

High-resolution four-dimensional carbon-correlated ^{1}H–^{1}H ROESY experiments employing isotags and the filter diagonalization method for effective assignment of glycosidic linkages in oligosaccharides

Geoffrey S. Armstrong, Brad Bendiak *

Department of Cell and Developmental Biology and Biomolecular Structure Program, University of Colorado Health Sciences Center, Mail Stop 8108, P.O. Box 6511, Aurora, CO 80045, USA

Received 9 February 2006; revised 18 March 2006
Available online 18 April 2006

Abstract

Four-dimensional nuclear magnetic resonance spectroscopy of oligosaccharides that correlates ^{1}H–^{1}H ROESY cross peaks to two additional ^{13}C frequency dimensions is reported. The ^{13}C frequencies were introduced by derivatization of all free hydroxyl groups with doubly ^{13}C-labeled acetyl isotags. Pulse sequences were optimized for processing with the filter diagonalization method. The extensive overlap typically observed in 2D ROESY ^{1}H–^{1}H planes was alleviated by resolution of ROESY cross peaks in the two added dimensions associated with the carbon frequencies of the isotags. This enabled the interresidue ^{1}H–^{1}H ROESY cross peaks to be unambiguously assigned hence spatially proximate sugar spin systems across glycosidic bonds could be effectively ascertained. An experiment that selectively amplifies *interresidue* ROESY ^{1}H–^{1}H cross peaks is also reported. It moves the magnetization of an *intraresidue* proton normally correlated to a sugar H-1 signal orthogonally along the z axis prior to a Tr-ROESY mixing sequence. This virtually eliminates the incoherent intraresidue ROESY transfer, suppresses coherent TOCSY transfer, and markedly enhances the intensity of interresidue ROESY cross peaks.

Keywords: Filter diagonalization method; Multi-dimensional NMR; Constant-time; ^{13}C labeling; O-acetylation; Rotating-frame cross-relaxation; Oligosaccharides

1. Introduction

Carbohydrates play crucial roles in a number of cellular recognition events including ligand–receptor interactions during development and various cell adherence and signaling processes [1–4]. With glycoproteins, disruption of oligosaccharide biosynthetic pathways correlates with oncologic events, highlighting the need to rapidly and confidently determine the primary structures of the carbohydrate components [5]. In the past, oligosaccharides have been primarily investigated by NMR in D_2O solution [6–8]. For structures derived from natural sources, any sensitive correlation experiments are essentially restricted to ^{1}H–^{1}H couplings. However, their 2D ^{1}H–^{1}H spectra are notoriously difficult to assign because six out of seven of the sugar ring protons are found in an overlapped spectral precinct of less than 1 ppm in either dimension. While some of the protons can be assigned by TOCSY correlations to H-1 protons that are found downfield, magnetization transfer around the ring is often restricted at some point due to a small *J*-coupling. Two-dimensional ^{1}H–^{1}H NOESY or ROESY [8,9] experiments are usually difficult to fully assign due to spectral overlap. Moreover, interresidue ^{1}H–^{1}H assignments, when possible to make, are not

* Corresponding author. Fax: +1 303 724 3420.
E-mail address: Brad.Bendiak@UCHSC.edu (B. Bendiak).

1090-7807/$ - see front matter © 2006 Elsevier Inc. All rights reserved.
doi:10.1016/j.jmr.2006.03.017

necessarily the strongest between two protons directly across a glycosidic bond, hence glycosidic linkage positions cannot be established with certainty from interresidue NOESY or ROESY correlations.

We have previously demonstrated that by completely derivatizing complex carbohydrates with doubly ^{13}C-labeled acetyl groups (''isotags'') [10,11] five major advantages can be realized for the primary structure determination of carbohydrates: (1) The spectral range of the sugar ring proton signals is increased about 3-fold resulting in nearly a 9-fold increase in spectral area for ^{1}H–^{1}H correlations and far fewer strong couplings. (2) The 3-bond couplings (2.5–4.7 Hz) between the acetyl carbonyl carbons and the sugar ring protons at the site of acetylation easily establish the acetylation positions through simple hetCOSY correlations [10]. By inference, *locations of glycosidic linkages* on individual sugars are readily assigned, as acetylation and glycosidic linkage sites are mutually exclusive. This provides a simple alternative to a time-honored method for sugar linkage site determination (''permethylation analysis,'' [12]) previously performed to obtain the same information, but requiring complete oligosaccharide degradation. (3) The acetyl group nuclei can be correlated to sugar ring protons to provide up to three additional frequency dimensions. This markedly increases spectral resolution of the sugar protons. By maintaining purely absorptive in-phase magnetization transfer within each sugar proton spin system, the axial/equatorial relationships of the sugar ring protons can be determined around each monosaccharide [13]. Furthermore, with pyranosides, acetylation does not affect the sugar chair forms, so *J*-couplings are similar to underivatized molecules [10]. (4) Each monosaccharide spin system usually correlates to more than one set of acetyl group frequencies, which drastically reduces the chance that overlaps will exist in indirect dimensions for oligosaccharides having many spin systems. (5) Magnetization can be transferred into the sugar ring proton spin system from different sites. This greatly ameliorates the problem of having to correlate sugar ring protons to the H-1 in TOCSY transfers because the sugar ^{1}H–^{1}H correlations can be monitored starting from any of the acetylated positions around the sugar ring. Tailoring the pulse sequence to leverage the resolving power of the filter diagonalization method (FDM, [14,15]) enabled four-dimensional spectra to be acquired rapidly with far fewer points required in the indirect dimensions as compared to conventional Fourier transform or mirror-image linear prediction methods [13]. While the stereochemistry, anomeric configuration and site of linkage substitution for each monosaccharide can now be effectively determined using the aforementioned through-bond experiments, the problem of *which sugars are specifically linked to which* remains.

Establishing *interresidue* ^{1}H–^{1}H correlations between all sugar spin systems in oligosaccharides under isotropic conditions is often surprisingly difficult. Typically, any coherent correlations ($^{4}J_{H,H}$ and sometimes $^{5}J_{H,H}$) are weak [16,17]. Many oligosaccharides are in the intermediate tumbling regime where incoherent correlations via longitudinal cross-relaxation are either weak or vanish (where $\omega_0\tau_c = \sqrt{5/2}$). This was one original impetus for development of CAMELSPIN (ROESY) by Bothner-By et al. [8]. Both ROESY and NOESY correlations have been reported between sugars in unlabeled acetylated oligosaccharides [18,19]; the ROESY experiment is of course more generally applicable to oligosaccharides of varying molecular weight. The presence of unwanted cross peaks due to coherent intraresidue (TOCSY- and COSY-type) transfer during ROESY experiments is well known [9,20]. Fortunately, they can now be markedly suppressed with multiple-pulse elements (Tr-ROESY or MP-ROESY [21,22]) applied during mixing times to effectively remove these and zero-quantum effects. These pulse trains have markedly improved the fidelity of spectra, with assurance that cross peaks actually represent incoherent magnetization transfer.

Another problem, often less appreciated, is illustrated in Fig. 1, where data was taken from crystallographic, NMR, and computer modeling studies [23–29]. Intraresidue ^{1}H–^{1}H distances are usually less than those across the glycosidic bond. For example, for glycosides having either an axial or equatorial proton at position 2, either in α- or β-configuration, there is always a nearby intraresidue proton at a distance of 2.6 Å or less from the sugar H-1. This is either the H-2, or, for β-sugars, the H-3 and H-5 protons. This is most pronounced for a β-pyranoside having an equatorial H-2 such as a β-mannoside (Fig. 1), where three protons are nearby. The time-averaged proton distances between sugars across glycosidic linkages typically vary from 2.3–3.5 Å, depending on the glycosidic torsion angles ϕ and ψ. The maximum possible distance still maintaining a covalent linkage is near 4.2 Å and when such distances are approached NOE intensities are weak. Simply for the purposes of *assigning* interresidue adjacencies, maximal interresidue NOE buildup with highest sensitivity is sought, as opposed to measuring initial NOE buildup rates to calculate ^{1}H–^{1}H distances. As an NOE (or ROE) is dependent on r^{-6}, it is worth noting that in many cases the majority of the magnetization from an H-1 proton (over 90%) can transfer to intraresidue protons, often primarily to one of them, rather than to a proton or protons of an adjacent residue. A similar scenario results for the transfer of magnetization between protons in the opposite direction across the glycosidic bond, where simple calculations reveal that the majority of the magnetization for most sugars transfers to intraresidue protons. Here, we address this intraresidue ''siphoning'' of magnetization by significantly suppressing ROE transfer to the nearest intraresidue proton, which enables more magnetization to transfer to interresidue protons and hence markedly enhances interresidue ROESY cross peak intensities.

Finally, ROESY correlations are restricted to one ^{1}H–^{1}H plane and the same issues of spectral overlap occur in the acylated oligosaccharides as occur with the underivatized molecules, albeit with somewhat less congestion due to the increased proton dispersion. By bringing the advan-

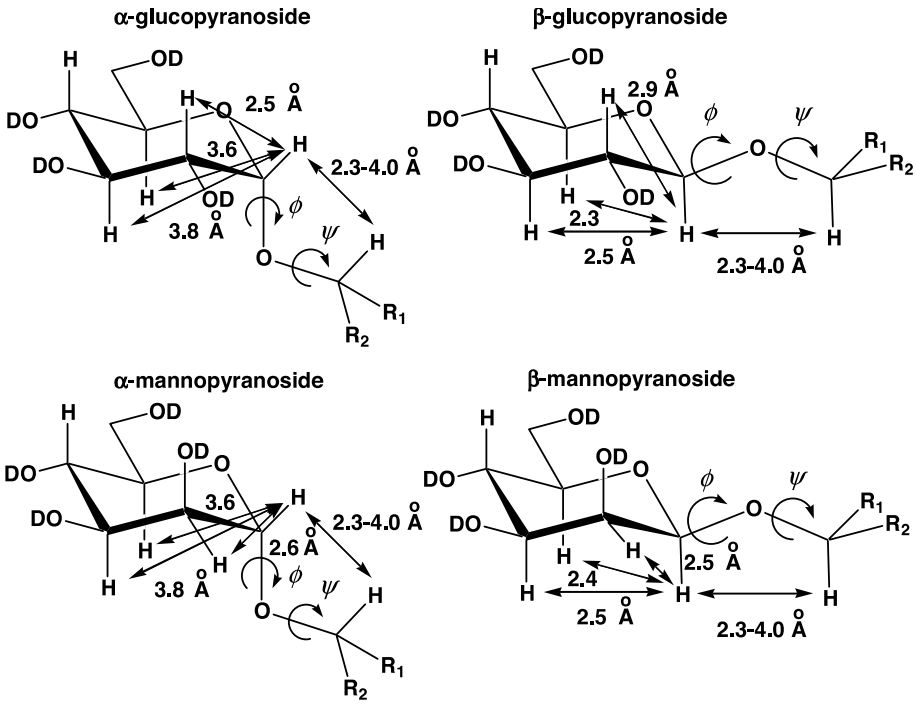

Fig. 1. Distances between protons in typical carbohydrate structures. Intraresidue distances and distances across the glycosidic bond are indicated for representative hexopyranosides having either an axial or equatorial hydroxyl group at C-2, for both anomeric configurations. All distances are shown as double-headed arrows between protons and are in Å. Angles (ϕ and ψ) illustrating rotational degrees of freedom about glycosidic bonds are indicated. Data are from a compilation of crystallographic, NMR, and computational modeling studies [23–29].

tages of isotags to bear on the assignment of interresidue ^{1}H–^{1}H correlations observed in ROESY experiments, connectivities between sugars can be resolved in additional dimensions through their correlation to isotag nuclear frequencies and the value of the FDM can be wielded to full advantage. In this paper, we present a four-dimensional experiment that enables the linkages between specific sugars of complex carbohydrates to be established, in combination with previous through-bond experiments to formally assign the positions of acetyl substitutions and the stereochemistry of individual monosaccharides [13,10]. The experiments enable the primary structure of complex carbohydrates to be determined with far greater confidence and efficacy.

2. Theory

The FDM [14,15] is a multi-dimensional data analysis technique that allows high-resolution spectral estimates to be constructed from temporally limited data sets. The theory of the method as applied to 4 dimensions has been presented previously in detail [13]; only a cursory description will be presented here. The major advantage of the method arises from the fact that in a multi-dimensional data set there is a relationship between each point in every dimension. Even though the data is acquired as a set of independent FIDs, the data is not transformed serially one orthogonal dimension at a time as in conventional methods. If one can mathematically describe the relationship between every point in related sets of time-domain data (the FIDs), then their relationship in the frequency domain is also known. In the case of the FDM, the relationship between each time-domain point is described by a multidimensional time evolution operator, the form of which is not necessarily known for each experiment, but which can be constructed in an appropriate basis by the time-domain points themselves. The relationship between the points in the frequency domain is represented through a mathematical eigenstructure employing the eigenvalues and eigenvectors of the operators. By obtaining the exact solution for these parameters, a multidimensional spectrum can be calculated directly from the complex multidimensional sinusoidal elements, with arbitrary digital resolution. In other words, the number of data points collected in any given dimension has no direct bearing on the final digital resolution of the spectrum in that dimension, as long as the total size of the multidimensional data set (product of the number of points in each dimension) is sufficiently large to accurately describe the relationships between the time-domain points.

In practice, the analysis of the time-domain data and the construction of a high-resolution spectrum is affected by several real-world limitations. This leads to a set of parameters that usually need to be adjusted in order to obtain a suitable result. The first problem is the size of a multi-dimensional time-domain data set. Even with the collection of just a few points in each indirectly detected dimension, their product, coupled with the large number of data points usually present in the directly acquired dimension, is quite large. While the resolving power of the FDM hinges on this

fact, it leads to a numerically intensive eigenvalue problem. This cannot be solved directly in a reasonable period of time. For this reason, the FDM can be broken into smaller frequency "windows," which can be calculated more rapidly and added together to give the final spectrum. This gives rise to the first adjustable parameter, K_{win}, or the number of basis functions included in each window. Practically speaking, this parameter is usually on the order of a few hundred basis functions to give decent spectral estimates in a reasonable amount of computational time. The size of the window can also be adjusted in each dimension individually, which can offer advantages in certain situations [30,31].

A second problem arises because the actual number of frequency components that give rise to a time-domain data set is unknown. This, coupled with the fact that noise in the signal cannot be effectively described by an evolution operator (there is no correlation between the time-domain points for noise), leads to uncertainty in the spectral representation of the data. Usually, this uncertainty manifests itself as sharp spurious artifacts distributed throughout the spectrum, where the linewidth of the spikes is determined by the final digital resolution of the spectrum. These can be markedly suppressed using a smoothing constraint in the solution of the eigenvalue problem [15], which requires the use of a regularization parameter, q, that must be adjusted manually based on the presence of the sharp artifacts in the resulting spectrum.

The presence of noise in the data may also have an effect on the accuracy of the spectral parameters determined by the method. In particular, the linewidths of the spectral features may be affected by noise. If the natural linewidth of a feature is small (or in the case of constant time data, zero) then small perturbations may lead to an arbitrary change in sign of its amplitude. For this reason, it is beneficial to apply a reasonable linebroadening, Γ, to the feature before the spectrum is constructed. This value is usually on the order of the natural linewidth of the peak under ideal sample conditions.

The final issue that arises is the physical memory space required for the multi-dimensional spectrum. As the spectrum can be constructed with arbitrary digital resolution, the product of the number of spectral points may end up being quite large. Since the spectrum is not constructed one dimension at a time, rather all at once, this entire frequency space must be held in memory until the calculation is complete. For this reason, the digital resolution that can be obtained in practice is in fact limited by the amount of memory available to the program. However, as higher-dimensional spectra have major regions that do not contain signals, it may be beneficial to construct high-resolution spectral estimates for small regions of focal interest, one at a time, rather than the entire spectrum.

3. Experimental

A pulse sequence (Fig. 2) was developed to transfer magnetization stepwise, starting from acetyl methyl protons, detecting indirectly on both ^{13}C nuclei of the isotags, then over to the protons of the sugar rings via a heteronuclear Hartmann–Hahn (HEHAHA) mixing period. It is well-known that the magnetization unavoidably transfers

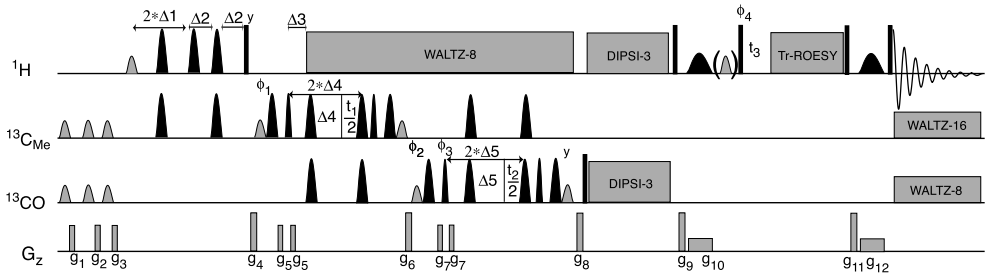

Fig. 2. Pulse sequence(s) for transfer of magnetization through the labeled nuclei of acetyl isotags to sugar ring protons followed by incoherent interresidue transfer: the 4D carbon-correlated Tr-ROESY experiments. The sequence was constant-time in indirect carbon dimensions (t_1 and t_2). The black rectangles are hard 90° pulses, the shaded rectangles indicate application of gradients. The small gray shaded curves represent shaped 90° pulses. All black curves represent shaped 180° pulses. The series of shaped pulses on either side of t_1 and t_2 were hyperbolic secant ABSTRUSE [35] pulse trains. All other 180° shaped pulses are BIP pulses [34]. The three shaped pulses on carbon at the beginning of the pulse sequence are hyperbolic secant pulses to remove native carbon magnetization. The first shaped 90° pulse on proton was an e-BURP [40] pulse, applied at the methyl proton frequency. The delays used are as follows: $\Delta1 = 3.8$ ms, $\Delta2 = 1.9$ ms, $\Delta3 = 1.5$ ms, $\Delta4 = 29.2$ ms, and $\Delta5 = 20.8$ ms. The DIPSI-3 [41,32,33,42] mixing sequence was applied at 2 kHz at the carbonyl and ring proton frequencies (9440 and −50 Hz, respectively) for 290 ms. These values were optimized empirically to affect the largest transfer of magnetization. After the DIPSI mixing sequence, the selective e-SNOB pulse (bracketed) [43] was applied conditionally at 100 Hz for 14.2 ms to sugar ring H-2 frequencies near 4.8 ppm to selectively move them along the z-axis, prior the Tr-ROESY [22] pulse train. This was applied at 5 kHz for 400 ms. Zero-quantum artifacts were removed in two places (during g_{10} and g_{12}) using a simultaneous 180° BIP pulse and gradient z-filter [36]. The first of these BIP pulses was applied at 65 kHz for 30 ms, the second at 12 kHz for 20 ms. WALTZ decoupling was applied on the carbon channel during acquisition. The decoupling was modulated to apply 1.375 kHz to the methyl frequency and 0.687 kHz to the carbonyl. On the diagram it has been represented as separate WALTZ-16 and WALTZ-8 sequences applied at each frequency. Gradients used in this sequence have the following values: $g_1 = 2.3$ G/cm, $g_2 = 2.3$ G/cm, $g_3 = 2.3$ G/cm, $g_4 = 11.5$ G/cm, $g_5 = 2.3$ G/cm, $g_6 = -16.1$ G/cm, $g_7 = 3.9$ G/cm, $g_8 = -18.4$ G/cm, $g_9 = 20.7$ G/cm, $g_{10} = 10.2$ G/cm, $g_{11} = -25.3$ G/cm, and $g_{12} = -1.9$ G/cm. Durations of the gradients were: g_1–$g_3 = 500$ μs; g_4, g_6, g_8, g_9, and $g_{11} = 400$ μs; g_5 and $g_7 = 200$ μs; g_{10} and g_{12}, 30 ms. Phase cycling was accomplished by alternating $\phi_3 = (x, y)$ and rec = (x, −x). Complex data was acquired using States-TPPI [44] incrementation of ϕ_1, ϕ_2, and ϕ_4. The number of points and spectral widths in each dimension are described in Section 3.

through the sugar proton spin system during a standard HEHAHA mixing period via homonuclear Hartmann–Hahn (HOHAHA) transfer [32,33]. The final step involves a Tr-ROESY transfer [21,22] to correlate sugar ring protons through-space to protons of adjacent sugar spin systems. Transfer steps are illustrated schematically in Fig. 3. The pulse sequence is a direct extension of the 4D constant-time pulse sequence presented previously [13], employing the additional multiple-pulse transverse rotating frame cross-relaxation mixing period. Overall magnetization transfer was optimized through the use of broadband inversion (BIP [34]) and ABSTRUSE [35] pulses. Purely absorptive in-phase magnetization was selected using an effective zero-quantum dephasing procedure [36]. The carbohydrate used was Nigeran tetrasaccharide (Sigma N7263, α-D-Glc-[1 → 3]-α-D-Glc-[1 → 4]-α-D-Glc-[1 → 3]-α-D-Glc). The compound was reduced with sodium borohydride to the alditol form before being acetylated with doubly ^{13}C-labeled acetic anhydride according to [10]. Data were collected on a Varian Inova 500 spectrometer equipped with a triple resonance gradient probe. The sample concentration was approximately 8 mM in $CDCl_3$ saturated with D_2O, allowing the ROESY data to be collected in 64 transients. Only two of the three acetyl group nuclei were indirectly observed in these experiments, the methyl carbon and carbonyl carbon, based on the spectral dispersion afforded by these nuclei. Three different sets of 4D experiments could be run leaving any one of the acetyl group nuclei out of the detection, but in the case of this molecule, two were sufficient to resolve the system. In the methyl carbon dimension, six points were collected with a spectral width of 150 Hz, 10 points were collected in the carbonyl carbon dimension with a spectral width of 200 Hz and 64 points in the indirect sugar ring proton dimension, with a spectral width of 1000 Hz. The experiment was constant-time in each of the carbon dimensions. In the direct dimension, a spectral width of 1000 Hz was used and 1024 data points were recorded. The data collection took 60 h. This time period was mainly required to obtain enough transients for moderate sensitivity of ROESY crosspeaks, not to improve resolution per se; other signals along the ^{1}H–^{1}H diagonal were easily observed. Data were processed using FDM software written in-house to apply the FDM algorithm to 4D data sets [13]. The spectral data was converted to NMRPipe [37] file format for visualization and further manipulation. All calculations were performed on an Apple PowerMac G5 with dual 2.5 GHz CPUs and 2 Mb RAM. The FDM calculation, using a single basis function per window[38] in the direct dimension ($K_{win} = 60$) took 3 h with this configuration. The remaining parameters for the FDM calculation were optimized at: $q^2 = 1 \times 10^{-4}$ and $\Gamma = 1$ Hz. The final 4D spectrum was digitized with 32 points in each of the carbon dimensions and 1024 and 64 points in each of the direct and indirect proton dimensions, respectively.

4. Results and discussion

4.1. Correlation of sugar ring ^{1}H–^{1}H Tr-ROESY cross peaks to acetyl ^{13}C frequencies in a single four-dimensional experiment processed with the filter diagonalization method

The 4D experiment outlined in Fig. 2 correlates two sugar ring ^{1}H–^{1}H dimensions through a basic Tr-ROESY mixing period with two of three possible dimensions defined by the frequencies of the acetyl isotags. When the experiment is performed using the ^{13}CO and $^{13}C_{Me}$ frequencies of the acetyl groups in indirect dimensions, it is preferable to initially analyze the data by viewing 2D projections of the 4D spectrum. For example, first a sugar spin system of interest can be selected from the ^{13}CO-direct proton projection (Fig. 4A). The purely absorptive in-phase nature of the multiplets enables the stereochemistry of the spin systems to be determined, as previously reported

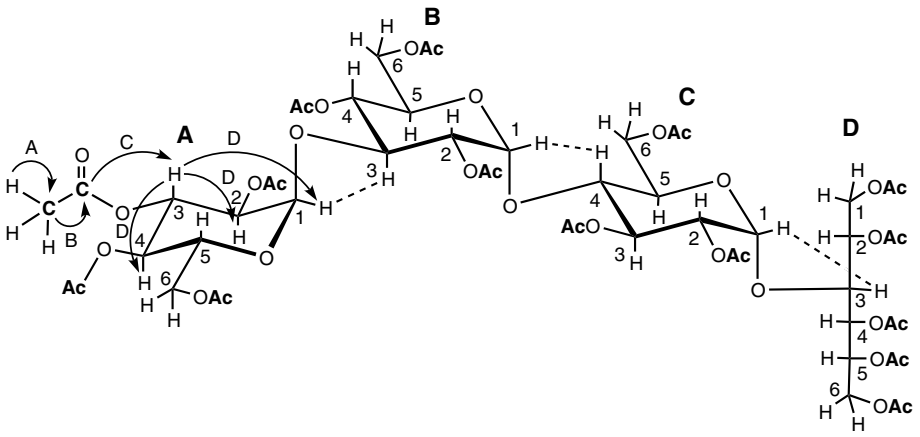

Fig. 3. The structure of the peracetylated nigeran tetrasaccharide-alditol, having doubly ^{13}C-labeled acetyl groups. Individual residues are indicated with large bold letters, and the numbering of carbons is shown for each sugar. Stepwise coherent magnetization transfers during the pulse sequence are shown as arrows, with each transfer indicated with a small letter: (A) INEPT transfer. (B) INEPT transfer. (C) heteronuclear Hartmann–Hahn transfer, which concurrently proceeds (in step D) through homonuclear Hartmann–Hahn transfer to other protons on the sugar. Incoherent ^{1}H–^{1}H transverse cross-relaxation correlations across glycosidic bonds are shown as dotted lines.

using a similar pulse sequence without the final Tr-ROESY step [13]. Once a spin system is identified (as in the boxed area in Fig. 4A), the ^{13}CO frequency can be read from the projected axis. Then the ^{13}CO–$^{13}C_{Me}$ projection (Fig. 4B) can be used to obtain the corresponding acetyl methyl carbon frequency. A 2D ^{1}H–^{1}H slice from the 4D spectrum that corresponded to these two carbon frequencies (Fig. 4C) was then selected and viewed. This allowed an independent 2D ^{1}H–^{1}H Tr-ROESY spectrum to be generated for each spin system, correlated to a pair of acetyl group ^{13}C frequencies "tagged" to that spin system. These 2D slices contain the ring proton signals for the representative spin systems as positive multiplets along the diagonal, with negative signals off the diagonal corresponding to Tr-ROESY correlations between protons through space. The greatest proton signal intensity was found along the diagonal of these 2D ^{1}H–^{1}H planes, as incoherent correlations were less sensitive. Contour levels are drawn at a relatively high threshold in Fig. 4C to illustrate the multiplet structures along the diagonal and to permit their comparison to the same spin system enclosed in the box in Fig. 4A.

The off-diagonal negative ROESY peaks are observed upon lowering the contour threshold (Fig. 5A) which obscures the diagonal peak multiplet structure. The same 2D plane is shown in Fig. 5A as was shown in Fig. 4C, at a much lower threshold in Fig. 5A. The Tr-ROESY signals fall into a few well defined regions because acetylation shifts all those sugar ring protons at acetylated positions downfield. Protons at positions not substituted with acetyl groups, with the exception of α-H1 signals, are upfield. Intraresidue ROESY cross peaks occurring between the H1 proton and protons at acetylated positions of the same sugar are downfield in both the direct and indirect proton dimensions. These signals can be easily discerned from the interglycosidic bond ROESY cross peaks, which occur between a downfield H1 and an upfield proton at the linkage position across the glycosidic bond. In addition, because the spin system has been isolated in multiple dimensions, no diagonal signal of an adjacent spin system is associated with the interglycosidic ^{1}H–^{1}H ROESY correlation. This makes identification of two sugars involved in a glycosidic linkage straightforward. The intensities of the interresidue ROESY cross peaks can vary markedly. In Fig. 5B, the cross peak between residue D H-3 and residue C H-1 is shown. It was far greater in intensity than was observed for the ROESY crosspeak between sugar residue

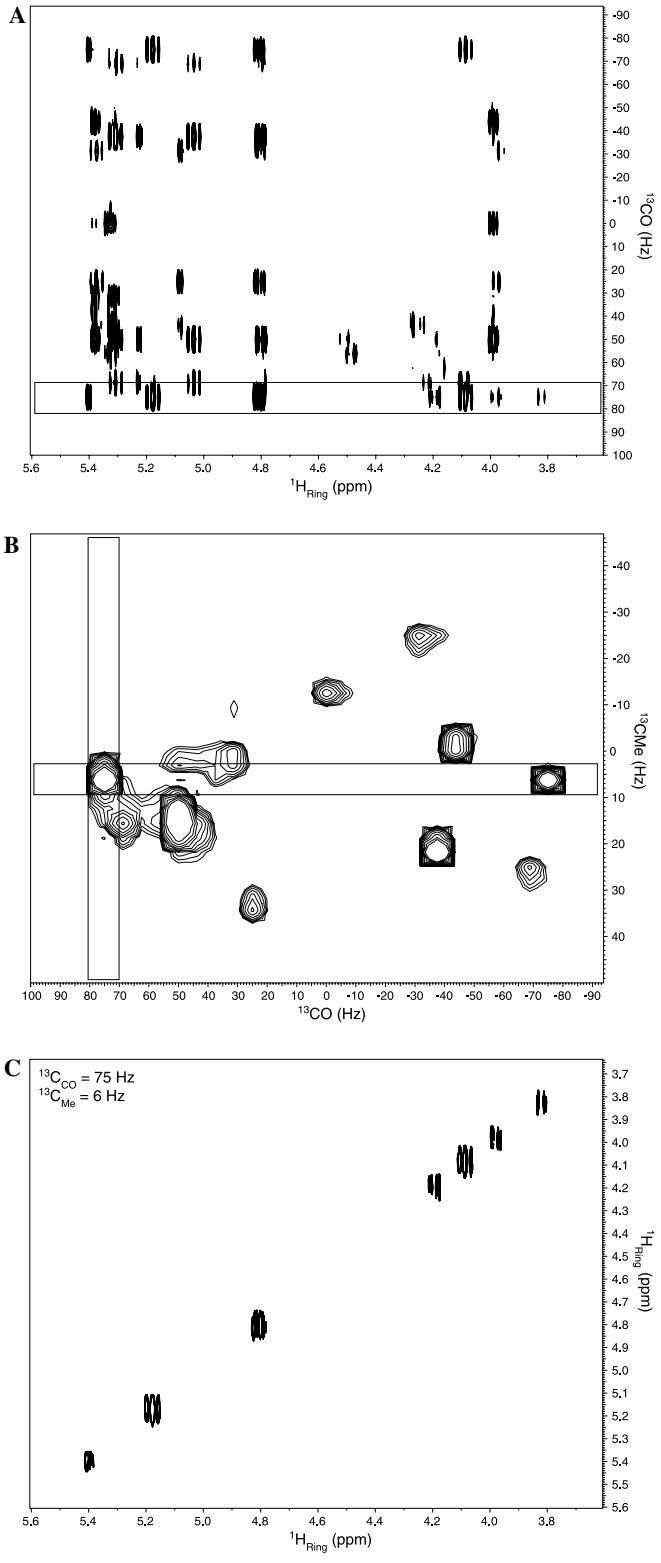

Fig. 4. Two-dimensional plots from the 4D experiment performed on the peracetylated nigeran tetrasaccharide-alditol having doubly ^{13}C-labeled acetyl groups. (A) The projection of the entire 4D data set onto the acetyl ^{13}CO-sugar ring ^{1}H plane. One spin system (residue B, Fig. 3) and part of another is shown within the boxed area. (B) The projection of the 4D data set onto the ^{13}CO–$^{13}C_{Me}$ plane. The region enclosed within both rectangular boxed areas corresponds to the frequencies of acetyl group carbons that correlate to the main proton spin system enclosed in the box in (A), and to the ^{1}H–^{1}H plane selected in (C). Cross peaks look "squarish" in some cases because they reflect the digital resolution afforded by the 4D experiment without additional manipulation or smoothing of data. (C) The ^{1}H–^{1}H plane that correlated to the acetyl group frequencies of 75 and 6 Hz along the ^{13}CO and $^{13}C_{Me}$ axes, respectively [bounded by both boxed regions in (B)]. The contour levels of this 2D slice were selected to show the couplings of signals along the diagonal. This illustrates the same spin system in two dimensions as is shown in the boxed region of (A).

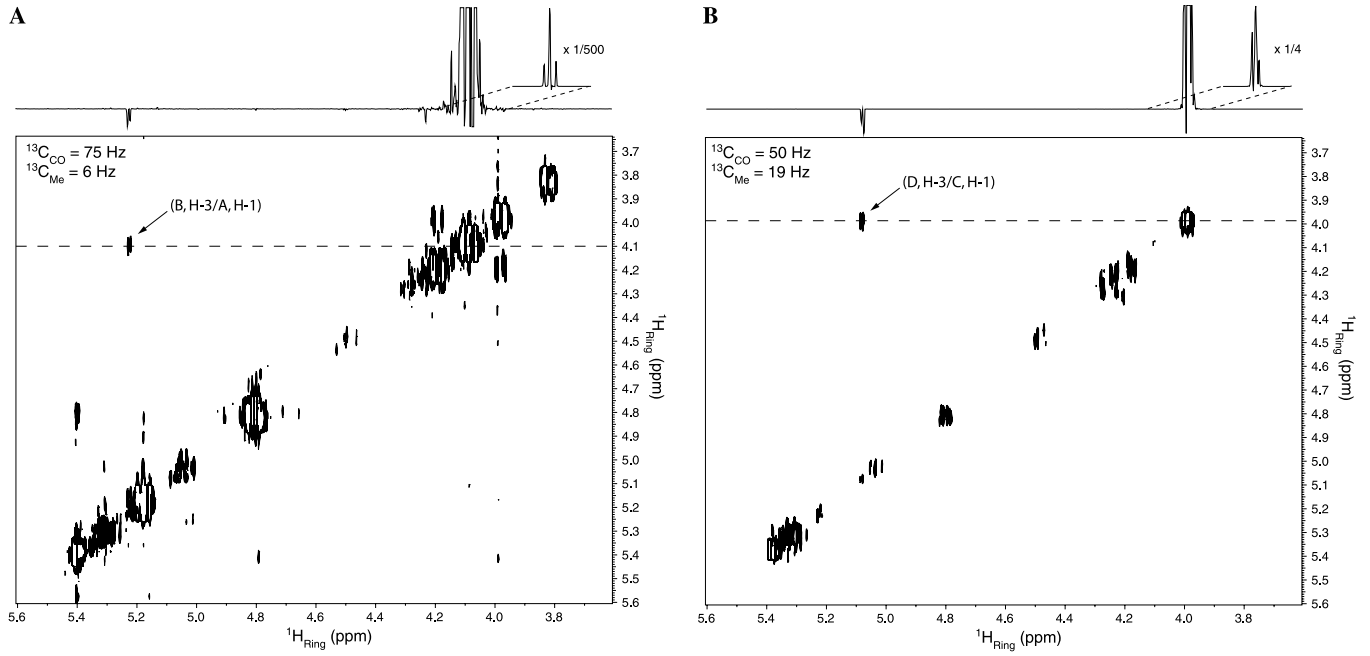

Fig. 5. Two-dimensional sugar ring ^{1}H–^{1}H Tr-ROESY planes representing individual sugar spin systems selected from the 4D experiment performed on the peracetylated nigeran tetrasaccharide-alditol having doubly ^{13}C-labeled acetyl groups. (A) The isolated ^{1}H–^{1}H plane that corresponds to acetyl group frequencies of 75 and 6 Hz along the CO and C_{Me} axes, respectively (as in Fig. 4C), shown at lower contour levels. The dashed line indicates an interresidue ROESY cross peak from sugar B H-3 to sugar A H-1 (Fig. 3). The 1D trace at this frequency is shown above the 2D plane, to indicate the relative intensities of the magnetization along the diagonal and the ROESY cross peak (the offset 1D region shows the diagonal at 1/500 intensity). (B) The isolated sugar ring ^{1}H–^{1}H plane that corresponds to acetyl group frequencies of 50 and 19 Hz along the CO and C_{Me} axes, respectively (see Fig. 4B). The dashed line indicates an interglycosidic Tr-ROESY cross peak from the sugar-alditol D H-3 to sugar C H-1 (Fig. 3). A 1D trace at this frequency is shown above the 2D plane (the offset 1D region shows the diagonal at 1/4 intensity). The ability to isolate individual sugar spin system ^{1}H–^{1}H planes from the 4D experiment enables interglycosidic ^{1}H–^{1}H ROESY correlations to be easily assigned.

B H-3 and A H-1 (compare traces and diagonal intensities of the 1D offsets in Figs. 5A and B).

Sensitivity of the Tr-ROESY signals is greatest from the linkage position proton (upfield) to the H1 proton of the previous ring as this signal is only split by the H1–H2 coupling. For this reason, it is beneficial to start assignment of the linkages at the reducing end of the oligosaccharide. This spin system is readily identifiable due to the lack of an H1 signal (as it has been reduced prior to acetylation). In the case of this tetrasaccharide, the 2D ^{1}H–^{1}H slice corresponding to methyl carbon and carbonyl carbon frequencies of 19 and 50 Hz, respectively, (that of the sugar-alditol D, Fig. 5B), showed an interresidue Tr-ROESY cross peak to an H1 signal at 5.08 ppm (that of sugar residue C). Selecting the spin system associated with this H1 frequency yielded a second 2D ^{1}H–^{1}H slice corresponding to methyl carbon and carbonyl carbon frequencies of 25 and −32 Hz respectively, having an interresidue Tr-ROESY cross peak to an H-1 at 5.4 ppm (that of sugar residue B). This then allowed the selection of a third 2D ^{1}H–^{1}H plane (Fig. 5A), with a methyl carbon frequency of 6 Hz and a carbonyl carbon frequency of 75 Hz, showing an interresidue Tr-ROESY cross peak to an H-1 at 5.23 ppm, the fourth and final ring of the tetrasaccharide. The final spin system (the non-reducing sugar, residue A, Fig. 3) showed no ROESY signals to other sugar H1 protons as expected. Using this straightforward approach, the linkages between each of the individual spin systems in the carbohydrate were unambiguously determined. By moving the planes of individual ^{1}H–^{1}H spin systems into additional dimensions defined by two of their isotag ^{13}C frequencies, interresidue ROESY assignments become simple. It is worth noting that without FDM processing the high resolution afforded in the indirect dimensions would not have been possible within a time period available between nitrogen fills.

4.2. Increasing the sensitivity of interglycosidic ^{1}H–^{1}H Tr-ROESY crosspeaks in the 4D experiment by suppressing key intraresidue transverse cross-relaxation pathways

An issue of unabated concern in making ROESY and NOESY correlations between protons across glycosidic linkages in carbohydrates is that the majority of the magnetization cross-relaxes preferentially from these to intraresidue protons. This often leads to low-intensity cross peaks both from the proton defined as the source and due to spin diffusion from the proton defined as the target. It would be beneficial in some cases, particularly where interresidue cross peaks are weak, to suppress the internal ROESY transfers to nearby correlated protons, forcing the ROESY to pursue a cross-linkage pathway. In the case of this tetrasaccharide, the strongest ROESY effects actually occur

between an α-glucoside H-1 and its own H-2 and between H-6a and H-6b.

The Tr-ROESY mixing sequence [21,22] was designed to virtually completely suppress TOCSY- and COSY-type effects during transverse cross-relaxation. The H-1 to H-2 Tr-ROESY transfer can also be eliminated quite readily as the signals for all of the H2 protons overlap near 4.8 ppm. By applying a selective 90° pulse at these frequencies before the Tr-ROESY mixing sequence (Fig. 2), the H2 protons are moved orthogonal to the cross-relaxation plane for the entire mixing pulse and do not undergo Tr-ROESY transfer. Based on the invariant trajectory approach [39], the cross-relaxation rates between a spin having an invariant trajectory and one orthogonal to it (i.e., originating and ending along one axis in the rotating frame versus the z-axis) approach zero during a multiple set of Tr-ROESY mixing cycles, within the frequency offset range used here.

The resultant enhancement in interresidue ROESY crosspeak intensity is shown in Fig. 6. Four-dimensional experiments were performed with (Fig. 6B) and without (Fig. 6A) a selective 90° pulse applied to the H-2 signals of the sugars at 4.8 ppm immediately prior to the Tr-ROESY mixing period. Although it is difficult to precisely quantitate the increase in magnetization transfer using the FDM, comparisons of the sugar B H-3/sugar A H-1 ROESY cross peak intensity to the sugar B H-3 diagonal intensity (Figs. 6A and B) indicate over a 10-fold improvement in sensitivity as compared to the experiment where the selective 90° pulse was not applied. This also resulted in excellent suppression of the H1–H2 intraresidue ROESY cross peaks (not shown), and increased the intensity of the

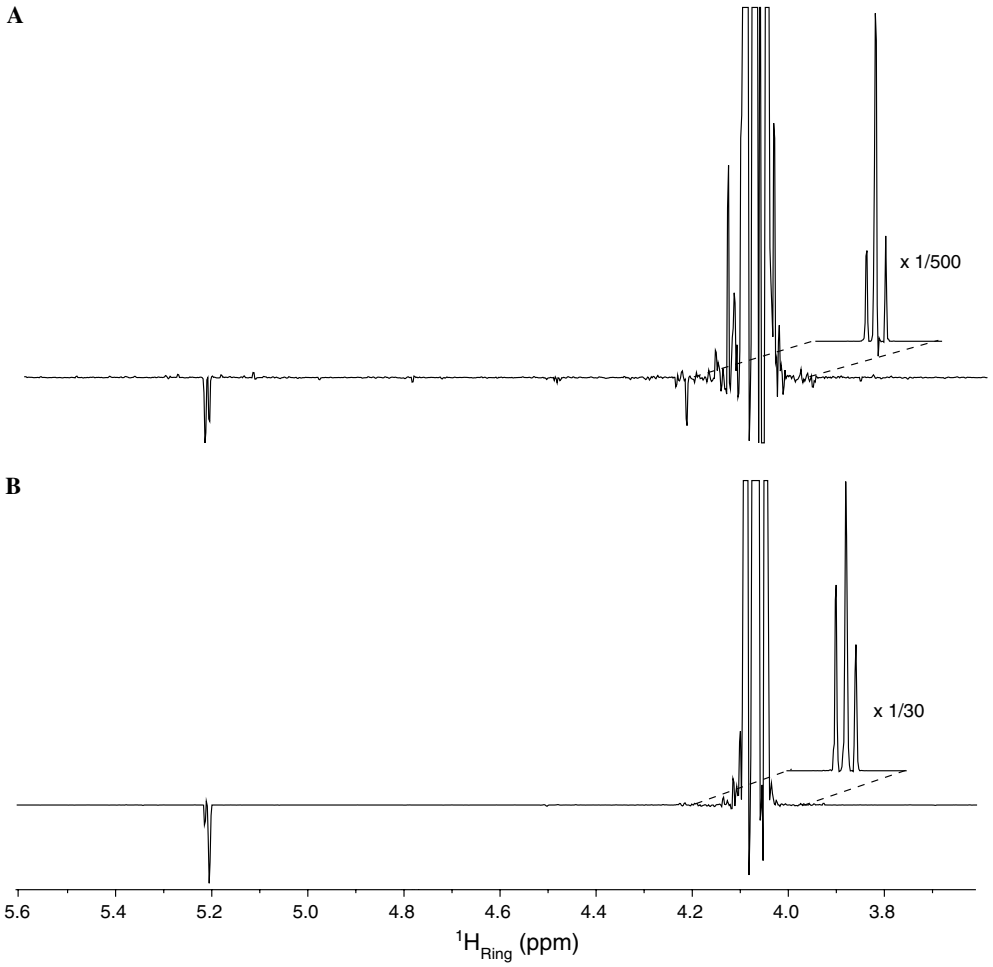

Fig. 6. Increasing the intensity of *interresidue* ROESY crosspeaks by eliminating *intraresidue* magnetization transfer within sugar spin systems during the Tr-ROESY step. A comparison is shown between data extracted from two related 4D spectra, performed on the peracetylated nigeran tetrasaccharide-alditol having doubly ^{13}C-labeled acetyl groups. Trace A: The standard 4D experiment with no selective pulse on the sugar H-2 signals. The trace was extracted from a 2D ^{1}H–^{1}H ROESY plane that shows a negative interglycosidic ROESY cross peak between a signal on the diagonal (the positive upfield H-3 signal of sugar residue B, Fig. 3) and the H-1 signal of residue A. This trace is the same as shown in Fig. 5A: the diagonal signal is shown in the 1D offset at 1/500 intensity. Trace B: The 4D experiment where the H-2 magnetization of all three cyclic sugars was selectively moved orthogonally using an e-SNOB pulse just prior to the application of the Tr-ROESY step. The 1D offset is shown at 1/30 intensity. Moving the sugar H-2 magnetization orthogonally with respect to the other protons for the period of the Tr-ROESY mixing sequence markedly increased the intensity of the interresidue ROESY crosspeak (about 10-fold) as compared to the intensity of the diagonal signal. This selectively blocked the rapid "siphoning" of magnetization to nearby H-2 protons, both from residue B H-3 to H-2 and from residue A H-1 to H-2 during the Tr-ROESY mixing time.

H1 to linkage proton ROESY cross peaks present upfield in the direct dimension and downfield in the indirect dimension, below the diagonal.

For this particular oligosaccharide, the α-glucoside H-2 positions were all acetylated and their signals coincidentally resonated downfield at a similar and unique frequency. However, it does not matter whatsoever if these H-2 signals happen to overlap with any other downfield signals of protons at acetylated positions: they can never be involved in a glycosidic linkage so eliminating any of these intraresidue ROESY pathways using a selective 90° pulse can only be beneficial. In brief, whenever an H-2 signal has a different chemical shift than the H-1 of the same spin system (i.e., they are not strongly coupled) this experiment can be used to intensify its interglycosidic cross peaks. This simply involves setting the offset of the selective 90° pulse prior to the Tr-ROESY, which will be unique to a given spin system within different oligosaccharides. The same argument applies to the elimination of any major intraresidue ROESY pathway occurring between any proton at a glycosidic linkage position and any proton at acetylated positions, which by nature resonate downfield. The concept of blocking certain pathways of cross-relaxation to intensify others should also be useful in applications to other molecules for measuring accurate ROESY buildup rates between distant protons experiencing major spin diffusion effects to nearby protons. This will be a topic of future studies using more appropriate spin system models.

4.3. Conclusions

This 4D Tr-ROESY experiment enables linkages between individual sugar subunits of a complex carbohydrate to be assigned much more effectively by spreading 2D ^{1}H–^{1}H ROESY planes of individual spin systems into more dimensions associated with the acetyl isotags. The FDM allows the 4D data to be acquired with fewer increments in indirect dimensions. Because the spin systems are isolated in multi-dimensional frequency space, the analysis of the data following FDM processing is straightforward. While in principle this experiment could be easily extended to 5D merely by observing on all of the acetyl group nuclei, the low inherent sensitivity of ROESY transfer across some glycosidic linkages results in an experimental time that is probably too great for this to be routinely feasible. It is worth noting that although an 8 mM solution was used for these 4D experiments, ROESY signals were readily detected over noise hence sample concentrations and times could be significantly decreased. Also, the probe we used had approximately a 750/1 signal/noise ratio with 0.1% ethyl benzene, whereas current cryoprobes are quoted above 4000/1. Acetylated oligosaccharides are very soluble in $CDCl_3$, so certainly lower-volume probes with mass-limited samples at higher concentrations would also be advantageous for improving sensitivity. Moreover, the particular structure used herein, where $\omega_0\tau_c$ was close to $\sqrt{5/2}$, is a worst-case scenario, absolutely requiring the ROESY transfer; for larger structures this can be replaced with a NOESY transfer step where mixing times can be lowered for higher sensitivity, as previously noted empirically with oligosaccharides [45]. In cases where interresidue ROE sensitivity is low at certain glycosidic linkage positions, selective elimination of key intraresidue transfers can markedly increase these crosspeak intensities. Such experiments have to be set up with a different offset of the final selective 90° pulse for those linkages having weak interglycosidic ^{1}H–^{1}H correlations for different oligosaccharides. They would be best initially performed as three dimensional variants to determine the frequencies of the weakly interacting interglycosidic proton pairs, then run in four dimensions if assignments prove difficult. Purely for the purposes of assigning interresidue ROESY proton pairs, in its 4D form, there are still three different experiments that can be performed, omitting observation on any one of the acetyl group nuclei. This experiment, coupled with the use of isotags and other assignment techniques described earlier [13,10] enables the stereochemistries, sites of linkage substitutions, and specific sugars involved in glycosidic linkages of complex carbohydrates to be determined far more effectively. Once set up, the FDM is of great practical value in generating high-resolution spectra in the indirect dimensions that would otherwise be impossible to accomplish in any reasonable period of time.

Acknowledgments

This research was supported by NSF Grant MCB-0236103. Helpful discussions with A.J. Shaka concerning Tr-ROESY and FDM processing are acknowledged.

References

[1] T. Hennet, L.G. Elies, Remodeling of glycoconjugates in mice, Biochim. Biophys. Acta 1473 (1999) 123–136.
[2] H.J. Gabius, S. Andre, H. Kaltner, H.C. Siebert, The sugar code: functional lectinomics, Biochim. Biophys. Acta (2002) 165–177.
[3] R.E. Hileman, J.R. Fromm, J.M. Weiler, R.J. Linhardt, Glycosaminoglycan-protein interactions: definition of consensus sites in glycosaminoglycan-binding proteins, Bioessays (1998) 156–167.
[4] K. Bruckner, L. Perez, H. Clausen, S. Cohen, Glycosyltransferase activity of Fringe modulates Notch–Delta interactions, Nature 406 (2000) 411–415.
[5] E.F. Hounsell, M. Young, J. Davies, Glycoprotein changes in tumours: a renaissance in clinical applications, Clin. Sci. 93 (1997) 287–293.
[6] J.P. Kamerling, J.F.G. Vliegenthart, High-resolution ^{1}H-nuclear magnetic resonance spectroscopy of oligosaccharide-alditols released from mucin-type *O*-glycoproteins, Biol. Magn. Reson. 10 (1993) 1–194.
[7] C.A. Bush, M. Martin-Pastor, A. Imberty, Structure and conformation of complex carbohydrates of glycoproteins, glycolipids and bacterial polysaccharides., Ann. Rev. Biophys. Biomol. Struct. 28 (1999) 269–293.
[8] A.A. Bothner-By, R.L. Stephens, J. Lee, C.D. Warren, R.W. Jeanloz, Structure determination of a tetrasaccharide: transient nuclear Overhauser effects in the rotating frame, J. Am. Chem. Soc. 106 (1984) 811–813.

[9] A. Bax, D.G. Davis, Practical aspects of two-dimensional transverse NOE spectroscopy, J. Magn. Reson. 63 (1985) 207–213.
[10] B. Bendiak, T.T. Fang, D.N.M. Jones, An effective strategy for structural elucidation of oligosaccharides through NMR spectroscopy combined with peracetylation using doubly ^{13}C-labeled acetyl groups, Can. J. Chem. 80 (2002) 1032–1050.
[11] D.N.M. Jones, B. Bendiak, Novel multi-dimensional heteronuclear NMR techniques for the study of ^{13}C-O-acetylated oligosaccharides: expanding the dimensions for carbohydrate structures, J. Biomol. NMR 15 (1999) 157–168.
[12] B. Lindberg, J. Lonngren, Methylation analysis of complex carbohydrates: general procedure and application for sequence analysis, Methods Enzymol. 50 (1978) 3–33.
[13] G.S. Armstrong, V.A. Mandelshtam, A.J. Shaka, B. Bendiak, Rapid high-resolution four-dimensional NMR spectroscopy using the filter diagonalization method and its advantages for detailed structural elucidation of oligosaccharides, J. Magn. Reson. 173 (2005) 160–168.
[14] V.A. Mandelshtam, FDM: the filter diagonalization method for data processing in NMR experiments, Prog. NMR. Spec. 38 (2001) 159–196.
[15] J. Chen, V.A. Mandelshtam, A.J. Shaka, Regularization of the filter diagonalization method: FDM2K, J. Magn. Reson. 146 (2000) 363–368.
[16] G. Batta, A. Liptak, Long-range ^{1}H–^{1}H spin–spin couplings through the interglycosidic oxygen and the primary structure of oligosaccharides as studied by 2D-NMR, J. Am. Chem. Soc. 106 (1984) 248–250.
[17] A. Otter, D.R. Bundle, Long-range ^{4}J and ^{5}J, including interglycosidic correlations in gradient-enhanced homonuclear COSY experiments of oligosaccharides, J. Magn. Reson. B 109 (1995) 194–201.
[18] S. Gasa, M. Nakamura, A. Makita, M. Ikura, K. Hikichi, Complete structural analysis of globoseries glycolipids by two-dimensional nuclear magnetic resonance, Eur. J. Biochem. 155 (1986) 603–611.
[19] J. Dabrowski, A. Ejchart, R. Bruntz, H. Egge, Sequencing of peracetylated oligosaccharides by rotating-frame nuclear Overhauser enhancement spectroscopy, FEBS Lett. 246 (1989) 229–232.
[20] D. Neuhaus, J. Keeler, "False" transverse NOE enhancements in CAMELSPIN spectra, J. Magn. Reson. 68 (1986) 568–574.
[21] T.L. Hwang, A.J. Shaka, Cross relaxation without TOCSY: transverse rotating-frame Overhauser effect spectroscopy, J. Magn. Reson. 114 (1992) 3157–3159.
[22] T.L. Hwang, A.J. Shaka, Multiple-pulse mixing sequences that selectively enhance chemical exchange or cross-relaxation peaks in high-resolution NMR spectra, J. Magn. Reson. 135 (1998) 280–287.
[23] G.A. Jeffrey, S. Takagi, The crystal and molecular structure of methyl β-D-glucopyranoside hemihydrate, Acta Cryst. B 33 (1977) 738–742.
[24] G.A. Jeffrey, R.K. McMullan, S. Takagi, A neutron diffraction study of the hydrogen bonding in the crystal structures of methyl-α-D-mannopyranoside and methyl α-D-glucopyranoside, Acta Cryst. B 33 (1977) 728–737.
[25] P. de Waard, B.R. Leeflang, J.F.G. Vliegenthart, R. Boelens, G.W. Vuister, R. Kaptein, Application of 2D and 3D NMR experiments to the conformational study of a diantennary oligosaccharide, J. Biomol. NMR 2 (1992) 211–226.
[26] A. Kjellberg, G. Widmalm, A conformational study of the vicinally branched trisaccharide β-D-Glc*p*-(1-2)-β-D-Glc*p*-(1-3)-α-D-Man*p*-OMe by nuclear Overhauser effect spectroscopy and transverse rotating-frame Overhauser effect spectroscopy (TROESY) experiments: comparison to Monte Carlo and Langevin dynamics simulations, Biopolymers 50 (1999) 391–399.
[27] H. Neubauer, J. Meiler, W. Peti, C. Griesinger, NMR structure determination of saccharose and raffinose by means of homo- and heteronuclear dipolar couplings, Helv. Chim. Acta 84 (2001) 243–258.
[28] E.W. Sayers, J.W. Prestegard, Conformation of a trimannoside bound to mannose-binding protein by nuclear magnetic resonance and molecular dynamics simulations, Biophys. J. 82 (2002) 2683–2699.
[29] A. Imberty, S. Gerber, V. Tran, S. Perez, Data bank of 3-dimensional structures of disaccharides, a tool to build 3-D structures of oligosaccharides. 1. oligo-mannose type *N*-glycans, Glycoconj. J. 7 (1990) 27–54.
[30] V.A. Mandelshtam, The multidimensional filter diagonalization method. I. theory and numerical implementation, J. Magn. Reson. 144 (2000) 343–356.
[31] V.A. Mandelshtam, H.S. Taylor, A.J. Shaka, Application of the filter diagonalization method to one- and two-dimensional NMR spectra, J. Magn. Reson. 133 (1998) 304–312.
[32] L.R. Brown, B.C. Sanctuary, Hetero-TOCSY experiments with WALTZ and DIPSI mixing sequences., J. Magn. Reson. 91 (1991) 413–421.
[33] M. Ernst, C. Griesinger, R.R. Ernst, W. Bermel, Optimized heteronuclear cross polarization in liquids, Mol. Phys. 74 (1991) 219–252.
[34] M.A. Smith, H. Hu, A.J. Shaka, Improved broadband inversion performance for NMR in liquids, J. Magn. Reson. 151 (2001) 269–283.
[35] K.E. Cano, M. Smith, A.J. Shaka, Adjustable, broadband, selective excitation with uniform phase, J. Magn. Reson. 155 (2002) 131–139.
[36] M.J. Thrippleton, J. Keeler, Elimination of zero-quantum interference in two-dimensional NMR spectra, Angew. Chem. Int. Ed. 42 (2003) 3938–3941.
[37] F. Delaglio, S. Grzesiek, G.W. Vuister, G. Zhu, J. Pfeifer, A. Bax, NMRPipe: a multidimensional spectral processing system based on UNIX pipes, J. Biomol. NMR 6 (1995) 277–293.
[38] G.S. Armstrong, B. Bendiak, The single basis filter diagonalization method: a rapid multidimensional data processing scheme, J. Magn. Reson. 174 (2005) 163–170.
[39] C. Griesinger, R.R. Ernst, Cross relaxation in time-dependent nuclear spin systems: invariant trajectory approach, Chem. Phys. Lett. 152 (1988) 239–247.
[40] H. Geen, R. Freeman, Band selective radiofrequency pulses, J. Magn. Reson. 93 (1991) 93–141.
[41] A.J. Shaka, C.J. Lee, A. Pines, Iterative schemes for bilinear operators—application to spin decoupling, J. Magn. Reson. 77 (1988) 274–293.
[42] A. Majumdar, H. Wang, R.C. Morshauser, E.R.P. Zuiderweg, Sensitivity improvement in 2D and 3D HCCH spectroscopy using heteronuclear cross-polarization, J. Biomol. NMR 3 (1993) 387–397.
[43] E. Kupče, J. Boyd, I. Campbell, Short selective pulses for biochemical applications, J. Magn. Reson. B 106 (1995) 300–305.
[44] D. Marion, M. Ikura, R. Tschudin, A. Bax, Rapid recording of 2D NMR-spectra without phase cycling—application to the study of hydrogen-exchange in proteins, J. Magn. Reson. 85 (1989) 393–399.
[45] J.P.M. Lommerse, J.J.M. Van Rooijen, L.M.J. Kroon-Batenburg, J.P. Kamerling, J.F.G. Vliegenthart, Conformational analysis of two xylose-containing *N*-glycans in aqueous solution by using ^{1}H-NMR ROESY and NOESY spectroscopy in combination with MD simulations, Carbohydr. Res. 337 (2002) 2279–2299.